Bcl-2 and Bcl-x_L Suppress Glucose Signaling in Pancreatic β-Cells

Dan S. Luciani,[1,2,3] Sarah A. White,[1,2,3] Scott B. Widenmaier,[1] Varun V. Saran,[4,5] Farnaz Taghizadeh,[1] Xiaoke Hu,[1] Michael F. Allard,[4,5] and James D. Johnson[1,2]

B-cell lymphoma 2 (Bcl-2) family proteins are established regulators of cell survival, but their involvement in the normal function of primary cells has only recently begun to receive attention. In this study, we demonstrate that chemical and genetic loss-of-function of antiapoptotic Bcl-2 and Bcl-x_L significantly augments glucose-dependent metabolic and Ca^{2+} signals in primary pancreatic β-cells. Antagonism of Bcl-2/Bcl-x_L by two distinct small-molecule compounds rapidly hyperpolarized β-cell mitochondria, increased cytosolic Ca^{2+}, and stimulated insulin release via the ATP-dependent pathway in β-cell under substimulatory glucose conditions. Experiments with single and double Bax–Bak knockout β-cells established that this occurred independently of these proapoptotic binding partners. Pancreatic β-cells from Bcl-$2^{-/-}$ mice responded to glucose with significantly increased NAD(P)H levels and cytosolic Ca^{2+} signals, as well as significantly augmented insulin secretion. Inducible deletion of Bcl-x_L in adult mouse β-cells also increased glucose-stimulated NAD(P)H and Ca^{2+} responses and resulted in an improvement of in vivo glucose tolerance in the conditional Bcl-x_L knockout animals. Our work suggests that prosurvival Bcl proteins normally dampen the β-cell response to glucose and thus reveals these core apoptosis proteins as integrators of cell death and physiology in pancreatic β-cells. ***Diabetes*** **62:170–182, 2013**

Type 2 diabetes involves combined defects in β-cell function and mass. Therapeutic efforts to combat diabetes could benefit from a better understanding of proteins that control both β-cell physiology and apoptosis. Cell survival is tightly regulated by signaling pathways that converge on pro- and antiapoptotic proteins from the B-cell lymphoma 2 (Bcl-2) family. Prominent antiapoptotic members include Bcl-2, Bcl-x_L, and Mcl-1, whereas key apoptosis-inducing members include Bax, Bak, and the structurally distinct members Bad, Bid, and Bim (1,2). Elegant work from Danial et al. (3) demonstrated that Bad has a physiological role in β-cells, aside from its role in β-cell apoptosis. Specifically, Bad phosphorylated at serine 155 promotes glucose-stimulated insulin secretion via interactions with glucokinase (3). It is not known whether any other Bcl family members play roles in β-cell physiology. The best understood of the prosurvival proteins, Bcl-2 and Bcl-x_L, have been implicated in the control of β-cell survival under stress (4,5), but little is known about the roles of these proteins in healthy β-cells. Studies in other cell types have suggested that Bcl-2 and Bcl-x_L regulate Ca^{2+} homeostasis (6) and mitochondrial physiology (7,8). Given the unique roles for mitochondria and Ca^{2+} in β-cell glucose signaling, we hypothesized that prosurvival Bcl proteins may be important in normal β-cell function.

To date, most studies of antiapoptotic Bcl proteins in β-cells have relied on forced overexpression (9–11). In this study, we examined the roles of endogenous prosurvival Bcl proteins in pancreatic β-cells using complementary loss-of-function approaches, small molecule Bcl-2/Bcl-x_L antagonists, as well as Bcl-2 and Bcl-x_L knockout mice. Our results demonstrate the combined importance of Bcl-2 and Bcl-x_L for mitochondrial integrity and β-cell survival and reveal distinct roles for the endogenous proteins in metabolic signaling, Ca^{2+} homeostasis, and insulin secretion. Our findings place these important members of the core apoptotic machinery at the interface of β-cell survival and physiology.

RESEARCH DESIGN AND METHODS

Reagents. Compound-6 (also known as Bcl-2 inhibitor) and YC137 (also known as Bcl-2 inhibitor II) from Calbiochem (La Jolla, CA) were prepared in dimethyl sulfoxide. Fura-2/AM, Rhodamine123, and MitoTracker were from Life Technologies/Invitrogen (Burlington, Ontario, Canada). Propidium iodide (PI), nifedipine, diazoxide, sodium azide, and tetramethylrhodamine ethyl ester perchlorate (TMRE) were from Sigma-Aldrich (St. Louis, MO).

Imaging and flow cytometry. Dispersed islet cells and intact islets were imaged following 24–48 h culture on glass coverslips. Changes in cytosolic Ca^{2+}, mitochondrial membrane potential ($\Delta\Psi_m$), and NAD(P)H autofluorescence were imaged as described (12,13). Mitochondrial Ca^{2+}, endoplasmic reticulum (ER) Ca^{2+}, and the activation of caspase-3 were monitored in single MIN6 cells transfected with fluorescence resonance energy transfer (FRET)-based biosensors. MIN6 cell $\Delta\Psi_m$ was estimated using TMRE and flow cytometry (14). Late-stage cell death was imaged using PI (14).

Metabolism assays. To examine changes in the ATP/ADP ratio, MIN6 cells in 96-well plates were equilibrated for 30 min in Krebs Ringer Buffer (KRB) containing (in mM unless otherwise noted): 119 NaCl, 4.7 KCl, 25 $NaHCO_3$, 2.5 $CaCl_2$, 1.2 $MgSO_4$, 1.2 KH_2PO_4, 5 mg/mL radioimmunoassay-grade bovine albumin, and 3 mmol/L glucose, followed by treatment for 30 min as indicated. ATP/ADP ratios were measured using the ApoSENSOR kit (BioVision, Mountain View, CA) using a TECAN M1000 luminometer (Tecan Group Ltd.).

Glucose oxidation rates were determined in cultures of dispersed islet cells by quantifying $^{14}CO_2$ generated from metabolized ^{14}C-labeled glucose as described (15,16). Adherent islet cells in T-25 flasks were preincubated 1 h in 3 mmol/L glucose KRB. This was followed by 1 h incubation with KRB containing 1 μCi/mL [U-^{14}C]glucose and test concentrations of nonlabeled glucose during which $^{14}CO_2$ was collected in a hyamine trap. Injection of 9 N H_2SO_4 stopped the reaction and released $^{14}CO_2$ captured in the media as [^{14}C]bicarbonate. Flasks were gently agitated for 2 h at room temperature before measuring captured radioactivity using a Beckman LS6500 Liquid Scintillation Counter (Beckman Coulter). Glucose oxidation rates were normalized to total protein quantified from identical aliquots of similarly treated cells.

Mouse models. Bax$^{-/-}$ (Jax stock number 002994) and Bak$^{-/-}$ (Jax stock number 004183) mice and age- and background-matched wild-type controls were from The Jackson Laboratory (Bar Harbor, ME). Littermate Bcl-$2^{-/-}$,

From the [1]Department of Cellular and Physiological Sciences, University of British Columbia, Vancouver, British Columbia, Canada; the [2]Department of Surgery, University of British Columbia, Vancouver, British Columbia, Canada; the [3]Child & Family Research Institute, Vancouver, British Columbia, Canada; the [4]Department of Pathology and Laboratory Medicine, University of British Columbia, Vancouver, British Columbia, Canada; and the [5]University of British Columbia James Hogg Research Centre, St. Paul's Hospital, Vancouver, British Columbia, Canada.

Corresponding authors: James D. Johnson, jimjohn@mail.ubc.ca, and Dan S. Luciani, dluciani@cfri.ca.

Received 16 October 2011 and accepted 16 June 2012.

DOI: 10.2337/db11-1464

See accompanying commentary, p. 18.

Bcl-2$^{+/-}$, and Bcl-2$^{+/+}$ mice were obtained by breeding mice heterozygous for the Bcl2^{tm1Sjk} mutation (Jax stock number 002265; The Jackson Laboratory). To generate Bcl-x$^{flox/flox}$:Pdx1-CreER mice and Bcl-x$^{flox/flox}$ control littermates, we mated Pdx1-CreER mice (17) with Bcl-x$^{flox/flox}$ mice (exons 1 and 2 flanked by *Lox* P sites) (18). To create mice with double Bax and Bak deletion in their β-cells, we bred Pdx1-CreER animals with Bak$^{-/-}$:Bax$^{flox/flox}$ mice (Bax^{tm2Sjk}Bak1^{tm1Thsn}/J; Jax stock number 006329; The Jackson Laboratory) and obtained Bak$^{-/-}$:Bax$^{flox/flox}$:Pdx1-CreER and Bak$^{-/-}$:Bax$^{flox/flox}$ littermates. Ablation of Bcl-x and Bax was achieved by injecting Pdx1-CreER–positive animals and littermate controls with 3 mg/40 g of tamoxifen (Sigma-Aldrich) on 5 consecutive days. Glucose tolerance and in vivo insulin secretion were assessed following intraperitoneal injection with glucose as indicated. Insulin tolerance was assessed after intraperitoneal injection of 0.75 units/kg insulin. Animals were fasted for 6 h prior to study. Studies were approved by the University of British Columbia Animal Care Committee.

Islet isolation, cell culture, and insulin secretion. Mouse islet isolation by collagenase digestion/filtration and culture have been described (19). Human islets were obtained from Dr. Garth Warnock (Vancouver General Hospital) after consent and cultured as described (12). MIN6 cells were cultured in Dulbecco's modified Eagle's medium (25 mmol/L glucose). Insulin release was measured from dispersed mouse islet cells in 48-well plates (20). Cells were equilibrated for 60 min in 3 mmol/L glucose KRB and then stimulated for 45 min with treatments as indicated (20). Insulin secretion from batches of size-matched islets was examined by perifusion and radioimmunoassay as previously described (12).

Immunoblotting and coimmunoprecipitation. For immunoprecipitation, 500 μg of total protein was incubated overnight (4°C) with anti-Bad (catalog number 9292; Cell Signaling Technology; 1:200), followed by 3-h incubation (4°C) with protein A-agarose (Santa Cruz Biotechnology). Complexes were washed with PBS and protease inhibitors in Ultrafree-MC Filters (Millipore) and eluted using 4% SDS in PBS with protease inhibitors. In some studies, nuclear (PARIS; Ambion Inc.) and mitochondrial fractions (Mitochondrial/Cytosol Kit; BioVision, Inc.) were obtained. Proteins were resolved by SDS-PAGE, transferred to polyvinylidene difluoride membranes, and probed overnight (4°C) for Bcl-x_L, Bcl-2, Bax, cytochrome c (catalog numbers 2762, 2870, 2772, and 4272; Cell Signaling Technology); phospho-Bad Ser112, Ser136, and Ser155 (catalog numbers 9291, 4366, and 9297; Cell Signaling Technology), Bad, Bak (#06–536; Millipore), and Cre recombinase (Novagen).

Statistical analysis. Data are shown as mean ± SEM. Differences between two groups were compared by unpaired Student *t* test and multiple groups by one-way ANOVA followed by Bonferroni multiple comparison test. Differences were considered significant if $P < 0.05$.

RESULTS

Kinetic characterization of apoptotic events during prolonged Bcl-2/Bcl-x_L antagonism. We used small-molecule antagonists to probe moment-to-moment functions of Bcl-2 and Bcl-x_L in pancreatic β-cells. The structurally distinct inhibitors, compound 6 (C6) and YC137, were originally identified by their ability to bind both Bcl-2 and Bcl-x_L and displace proapoptotic members such as Bak and Bid (21,22). We first established that BH3-displacement could also be observed in intact β-cells. Indeed, C6 caused a rapid reduction in the amount of Bcl-x_L that was bound to the BH3-only protein Bad without affecting the total levels of Bad or Bcl-x_L protein within 1 h (Fig. 1*A* and *B*). This confirmed the expected mechanism of this antagonist on endogenous Bcl proteins in intact β-cells.

Displacement of BH3 domain proteins from Bcl-2 and Bcl-x_L by YC137 or C6 sensitizes tumor cells to apoptosis, an effect that is more potent with increasing Bcl-2 expression (21,22). Unlike many tumor cells, primary β-cells do not hyperexpress Bcl-2 or Bcl-x_L. We therefore tested if these inhibitors affect β-cell survival. Prolonged Bcl antagonism induced dose- and time-dependent cell death in human and mouse islet cells, as well as MIN6 β-cells (Fig. 1*C–E*). This involved mitochondrial apoptosis, as evidenced by redistribution of Bax from cytosol to mitochondria and release of mitochondrial cytochrome c (Fig. 1*F*). PI incorporation was preceded by the activation of caspase-3, imaged in real time (Fig. 1*G*). Of note, the $\Delta\Psi_m$ of β-cells treated with C6 or YC137 underwent an initial hyperpolarization that suggested mitochondrial activation within the first half hour, well prior to any evidence of apoptosis. This was followed hours later by collapse of $\Delta\Psi_m$, demonstrating a late-stage loss of mitochondrial integrity (Fig. 1*H*). These results demonstrate that even in the absence of other stresses, combined and sustained antagonism of Bcl-2 and Bcl-x_L initiates mitochondrial apoptosis in β-cells. Importantly, apoptosis was not detected earlier than 2 h, indicating that cellular responses occurring less than an hour after Bcl-2/Bcl-x_L antagonism are separate from the central apoptotic events.

Antagonizing Bcl-2/Bcl-x_L initiates K_{ATP} channel- and depolarization-dependent Ca^{2+} entry and insulin secretion. Remarkably, Bcl-2/Bcl-x_L antagonists rapidly triggered marked Ca^{2+} fluctuations in mouse and human islet cells that resembled Ca^{2+} responses to glucose (Fig. 2*A–C*). Similar effects were observed in MIN6 β-cells (Fig. 2*D*). The percentage of cells activated within 30 min of Bcl inhibition was concentration-dependent (Fig. 2*E*). The Ca^{2+} signals ceased upon washout of the inhibitor, strongly suggesting a physiological basis rather than cell damage. C6 also increased average cytosolic Ca^{2+} in intact islets, although the rapid fluctuations were dampened (Fig. 2*F*). Together, these findings provide the first direct evidence that prosurvival Bcl proteins regulate moment-to-moment calcium homeostasis in β-cells.

Next, we sought to determine the cellular site where Bcl-2 and/or Bcl-x_L control Ca^{2+} homeostasis. In other cell types, Bcl-2 and Bcl-x_L reside on the membranes of Ca^{2+} handling organelles, including the mitochondria, ER, and the nuclear envelope (23,24). The subcellular location of Bcl-2 and Bcl-x_L in β-cells has not been reported. We found that Bcl-2:GFP displayed some colocalization with mitochondria, but also had a clear nonmitochondrial distribution, likely reflecting ER (Fig. 3*A* and *D*). In contrast, Bcl-x_L:yellow fluorescent protein (YFP) showed near-exclusive colocalization with mitochondria, which at high magnification could often be seen in an apparent association with the mitochondrial membrane (Fig. 3*B* and *D*) and minimal association with ER (Fig. 3*C* and *D*). A differential distribution of endogenous Bcl-2 and Bcl-x_L between mitochondrial and nonmitochondrial compartments was also found by subcellular fractionation (Fig. 3*E*). These findings suggest that β-cell Bcl-2 and Bcl-x_L may have overlapping, but distinct, roles.

Bcl-2 and Bcl-x_L influence ER Ca^{2+} release in other cell types (6,25,26). Imaging ER luminal Ca^{2+} directly (14,27), we found that ER Ca^{2+} levels were not affected by C6 treatment for up to 50 min (Fig. 4*A*; similar results seen with 20–80 μmol/L C6). As a positive control, inositol triphosphate generation with carbachol consistently mobilized ER Ca^{2+} (Fig. 4*A*). Although these results suggest that acutely antagonizing Bcl-2 and Bcl-x_L does not alter β-cell ER Ca^{2+}, it remains possible that Bcl-2 or Bcl-x_L regulate β-cell ER Ca^{2+} homeostasis by mechanisms that are unaffected by these small-molecule antagonists.

Next, we sought to further elucidate the mechanism by which Bcl inhibitors increase cytosolic Ca^{2+}. Similar to stimulatory glucose, Bcl inhibitors had no effect on cytosolic Ca^{2+} in the absence of extracellular Ca^{2+} (Fig. 4*B*). Moreover, the L-type Ca^{2+} channel antagonist nifedipine reversibly lowered cytosolic Ca^{2+} during Bcl inhibition (Fig. 4*C*). Pretreatment of islet cells with nifedipine, the K_{ATP} channel agonist diazoxide, or a low dose of the mitochondrial uncoupler carbonyl cyanide *m*-chlorophenyl hydrazone (CCCP) prevented Ca^{2+} entry (Fig. 4*D*). Incubating islet cells with Bcl antagonist in the presence of

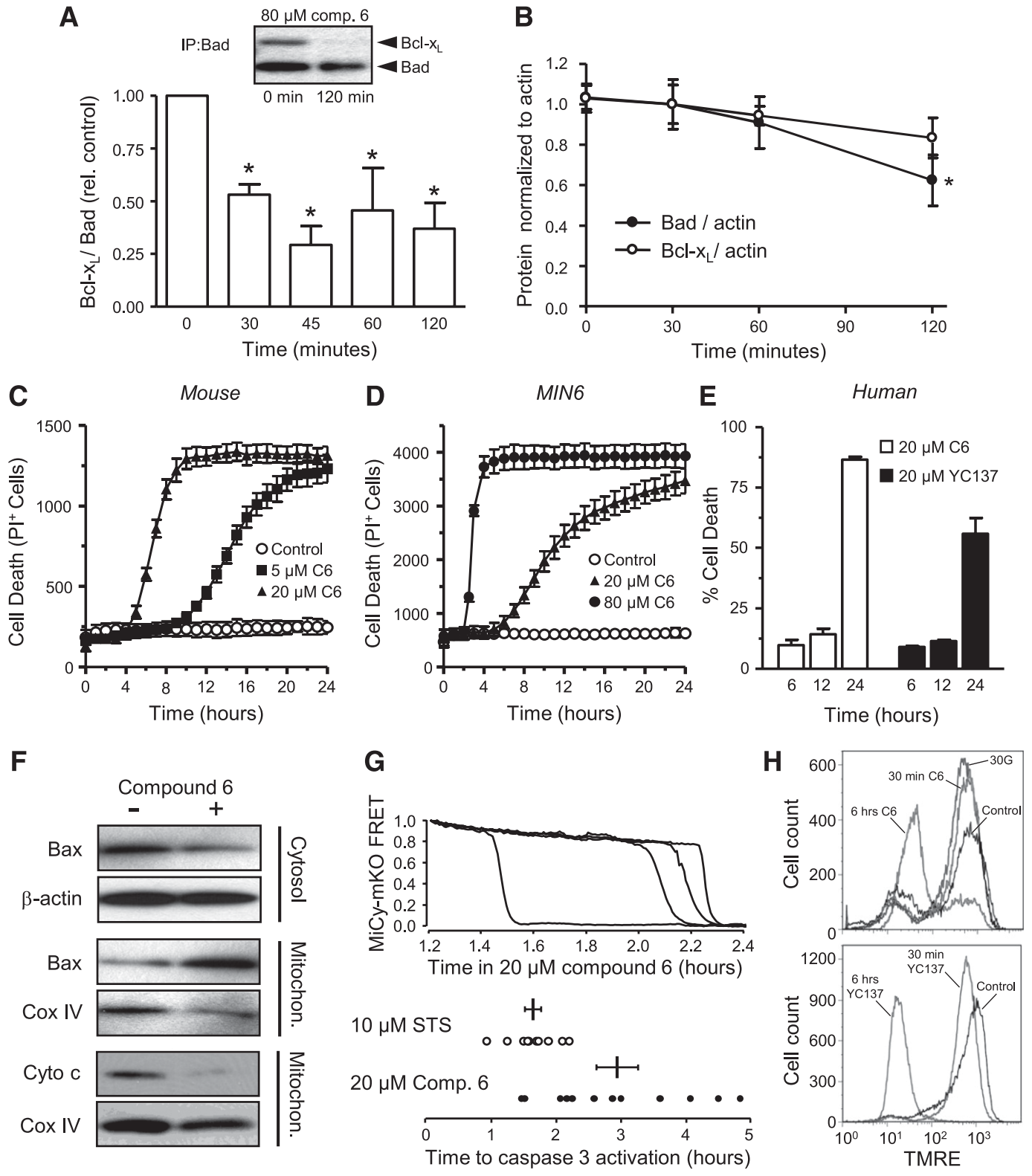

FIG. 1. Small-molecule inhibition of Bcl-2/Bcl-x_L rapidly displaces Bad and eventually induces mitochondrial apoptosis. *A*: *Top*: Western blot illustrating the loss of Bcl-x_L coimmunoprecipitation with Bad in MIN6 β-cells treated with C6. *Bottom*: Densitometric quantification of the ratio of Bcl-x_L to Bad protein in Bad immunoprecipitates after various durations of C6 exposure. Data (mean ± SEM) are normalized to control (n = 3–5; *P < 0.05 vs. time 0). *B*: Bcl-x_L and Bad protein levels in MIN6 β-cells treated with 80 μmol/L C6 (n = 3; *P < 0.05 vs. time 0). *C* and *D*: PI incorporation in mouse islet cells and MIN6 β-cells during incubation with C6 (n = 3). *E*: Relative cell death (PI$^+$ cells) in human islet cells treated with Bcl-2/Bcl-x_L antagonists (n = 3 donor preparations). *F*: Western blots for Bax and cytochrome c (Cyto c) in mitochondrial and cytosolic fractions from MIN6 β-cells treated with 40 μmol/L C6 for 4 h (n = 3). *G*: *Top*: Caspase-3 activation (loss of MiCy-mKO FRET) imaged in four individual MIN6 β-cells during continued Bcl-2/Bcl-x_L inhibition. *Bottom*: C6 (20 μmol/L) activated caspase-3 at an average time of 2.9 ± 0.3 h (n = 12 cells from two independent cultures). Staurosporine (STS; 10 μmol/L) activated caspase-3 after 1.65 ± 0.12 h (n = 10 cells from two independent cultures). *H*: Flow cytometric detection of mitochondrial membrane potential in MIN6 β-cells treated with 20 μmol/L C6, 20 μmol/L YC137, and 30 mmol/L glucose (30G). Reduction of TMRE intensity indicates a loss of $\Delta\Psi_m$ (n = 3 cultures). (A high-quality color representation of this figure is available in the online issue.)

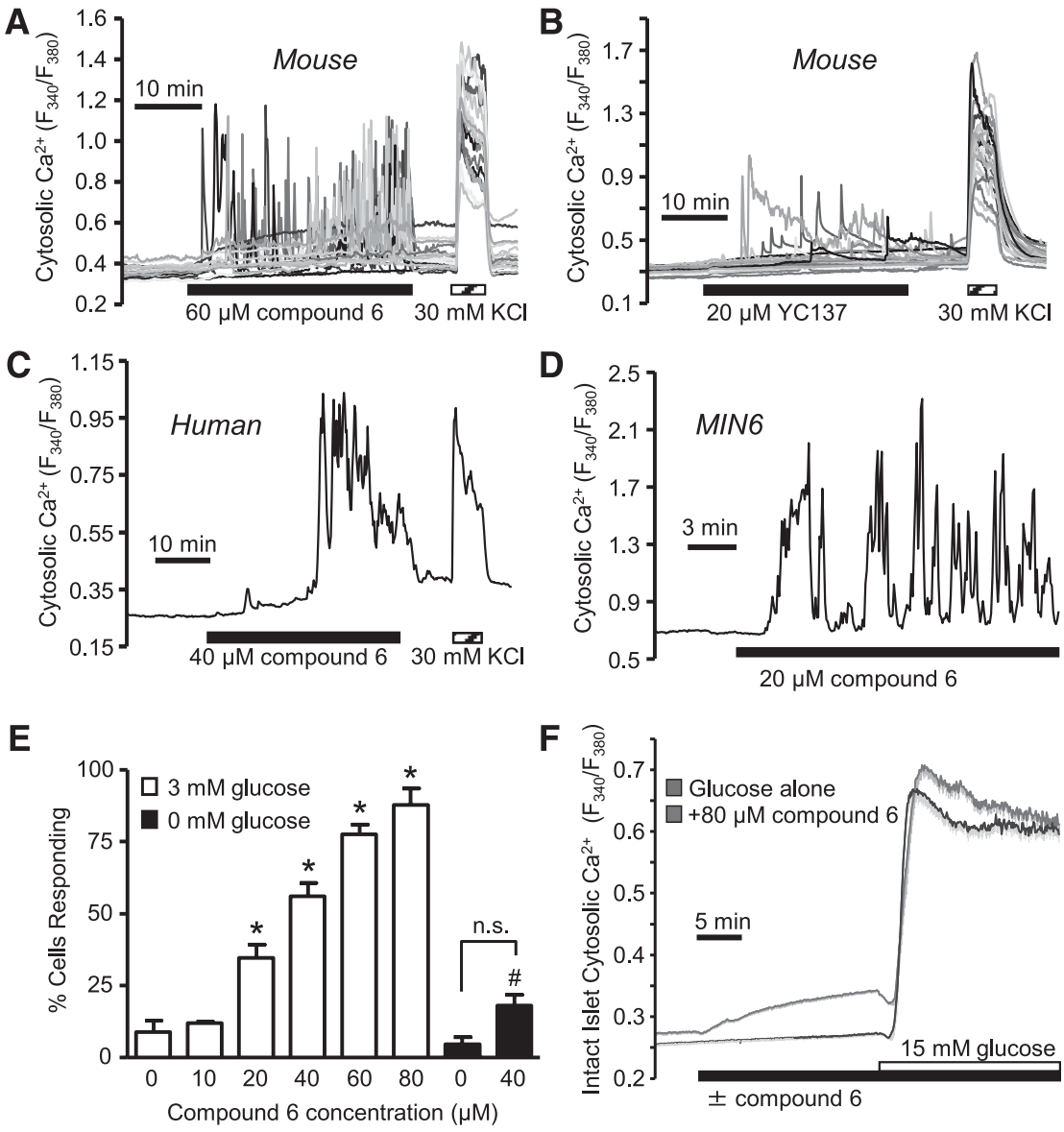

FIG. 2. Bcl-2/Bcl-x_L inhibition triggers cytosolic Ca^{2+} fluctuations. *A* and *B*: Cytosolic Ca^{2+} responses of groups of mouse islet cells exposed to Bcl-2/Bcl-x_L inhibitors C6 and YC137 in the presence of 3 mmol/L glucose. *C* and *D*: Representative cytosolic Ca^{2+} responses to C6 in human islet cells (n = 66 cells from three islet preparations) and MIN6 β-cells (n = 34 cells). *E*: Quantification of the percentage of baseline quiescent mouse islet cells that responded within 30 min to various doses of C6 in the presence of either 3 or 0 mmol/L glucose (n = 3–6 for each condition; *P < 0.05 vs. control in 3 mmol/L glucose, #P < 0.05 vs. 40 μmol/L C6 in 3 mmol/L glucose; n.s., not significant). *F*: Average cytosolic Ca^{2+} responses of intact pancreatic islets stimulated with 15 mmol/L glucose in the presence or absence of 80 μmol/L C6. Shaded hanging bars represent SEM (n = 12, n = 10). (A high-quality color representation of this figure is available in the online issue.)

substimulatory glucose (3 mmol/L) induced a modest, but significant, elevation in insulin release similar in magnitude to that triggered by 100 μmol/L of the K_{ATP} channel blocker tolbutamide (Fig. 4*E*). These insulin-secretion responses were attenuated by diazoxide and were not additive with the response to tolbutamide (Fig. 4*E*), or with a maximally stimulatory concentration of glucose (fold increase: 3.99 ± 1.12 in 20 mmol/L glucose vs. 3.44 ± 1.06 in 20 mmol/L glucose plus 40 μmol/L C6; n = 7; P = 0.73). Despite their ability to block the acute Ca^{2+} signals, nifedipine and diazoxide did not alter the degree or the kinetics of islet cell death induced by C6 (Fig. 4*F*). Together, these data demonstrate that antagonizing Bcl-2/Bcl-x_L acutely induces Ca^{2+} entry and insulin secretion from β-cells by mechanisms similar to those involved in glucose signaling (28) and that these physiological Ca^{2+} signals are not mechanistically related to the late-stage apoptotic effects of sustained Bcl-2/Bcl-x_L coinhibition.

Bcl-2/Bcl-x_L inhibition increases mitochondrial activity. Our results to this point indicated that the events induced by Bcl protein inhibition are similar to those that underlie β-cell glucose signaling. Indeed, sodium azide blocked C6-stimulated Ca^{2+} signals, establishing a requirement for mitochondrial respiratory flux (Fig. 4*G*). Importantly, Ca^{2+} signaling upon Bcl antagonism was suppressed in the absence of glucose (Fig. 2*E*), suggesting that a minimum of metabolic substrate is required to support the Ca^{2+} responses. These findings indicate that blocking Bcl-2/Bcl-x_L increases basal mitochondrial glucose metabolism rather than acting independently of the sugar.

To further establish if Bcl antagonists promote mitochondrial activity, we directly imaged $\Delta\Psi_m$ and mitochondrial Ca^{2+}

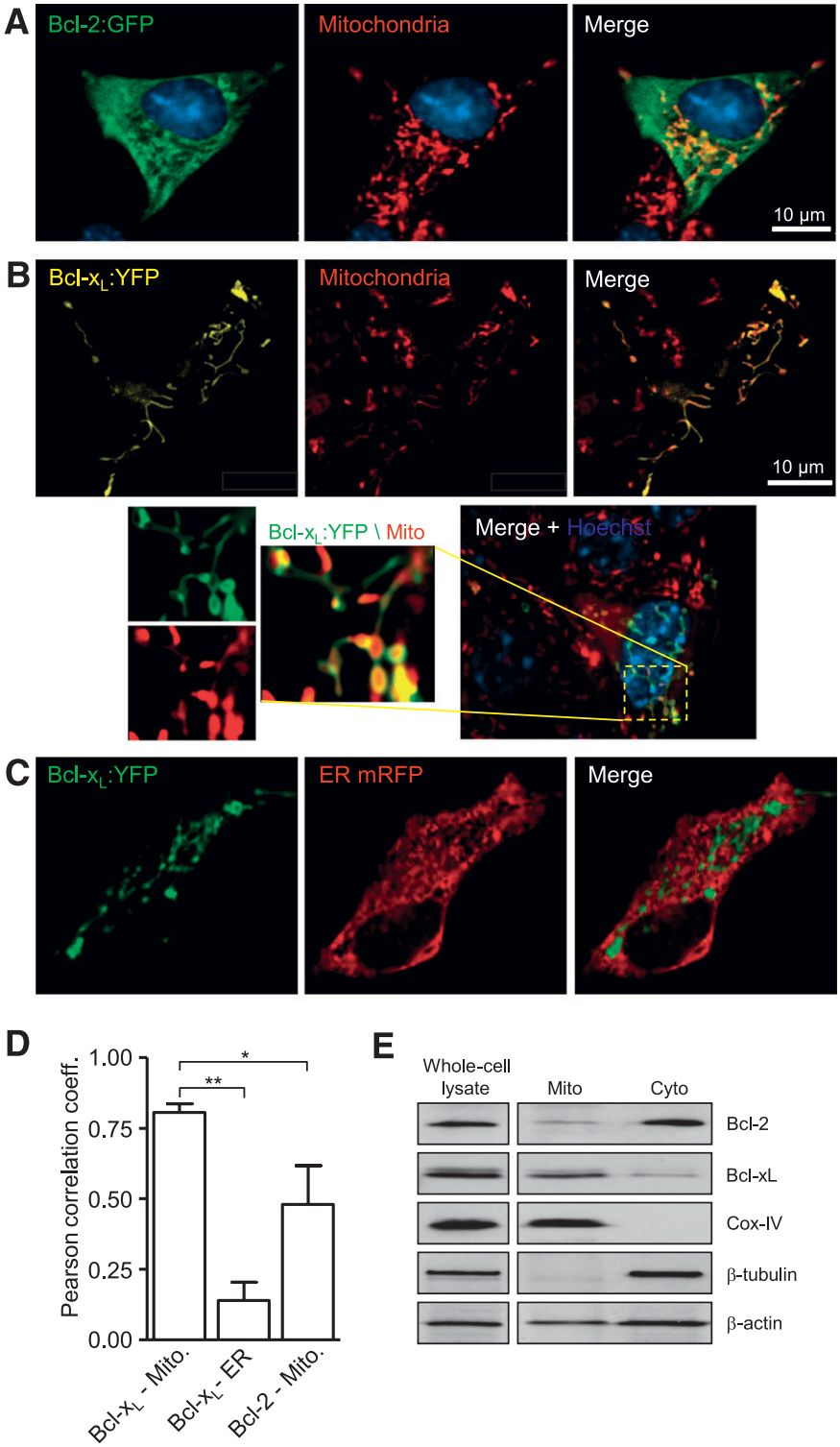

FIG. 3. Differential subcellular distribution of Bcl-2 and Bcl-x_L in β-cells. *A* and *B*: Representative images of MIN6 cells expressing GFP-tagged Bcl-2 and YFP-tagged Bcl-x_L and loaded with 100 nmol/L MitoTracker Red. *C*: MIN6 cell coexpressing Bcl-x_L:YFP and ER-targeted monomeric red fluorescent protein (mRFP). *D*: Pearson correlation coefficient (coeff.) quantifying colocalization of Bcl-x_L:YFP with mitochondrial dsRed ($n = 6$) or ER mRFP ($n = 5$) and Bcl-2:GFP with ER mRFP ($n = 5$) in MIN6 β-cells (*$P < 0.05$, **$P < 0.001$). *E*: Western blots for endogenous Bcl-2 and Bcl-x_L in fractions of MIN6 β-cells ($n = 3$). Cytochrome c oxidase (Cox-IV) indicates the mitochondrial fraction. (A high-quality digital representation of this figure is available in the online issue.)

(12,14,29). In agreement with our flow cytometry results, Bcl antagonism hyperpolarized the mitochondria of single primary mouse β-cells within minutes in a concentration-dependent manner (Fig. 4*H*). The $\Delta\Psi_m$ changes were comparable to the β-cell response to glucose, and the presence of Bcl-2/Bcl-x_L antagonist did not prevent additional glucose-induced hyperpolarization (Fig. 4*I*). Bcl-2/Bcl-x_L inhibition also evoked reversible mitochondrial Ca^{2+} signals that resembled glucose stimulation (Fig. 4*J*), providing further evidence for mitochondrial activation.

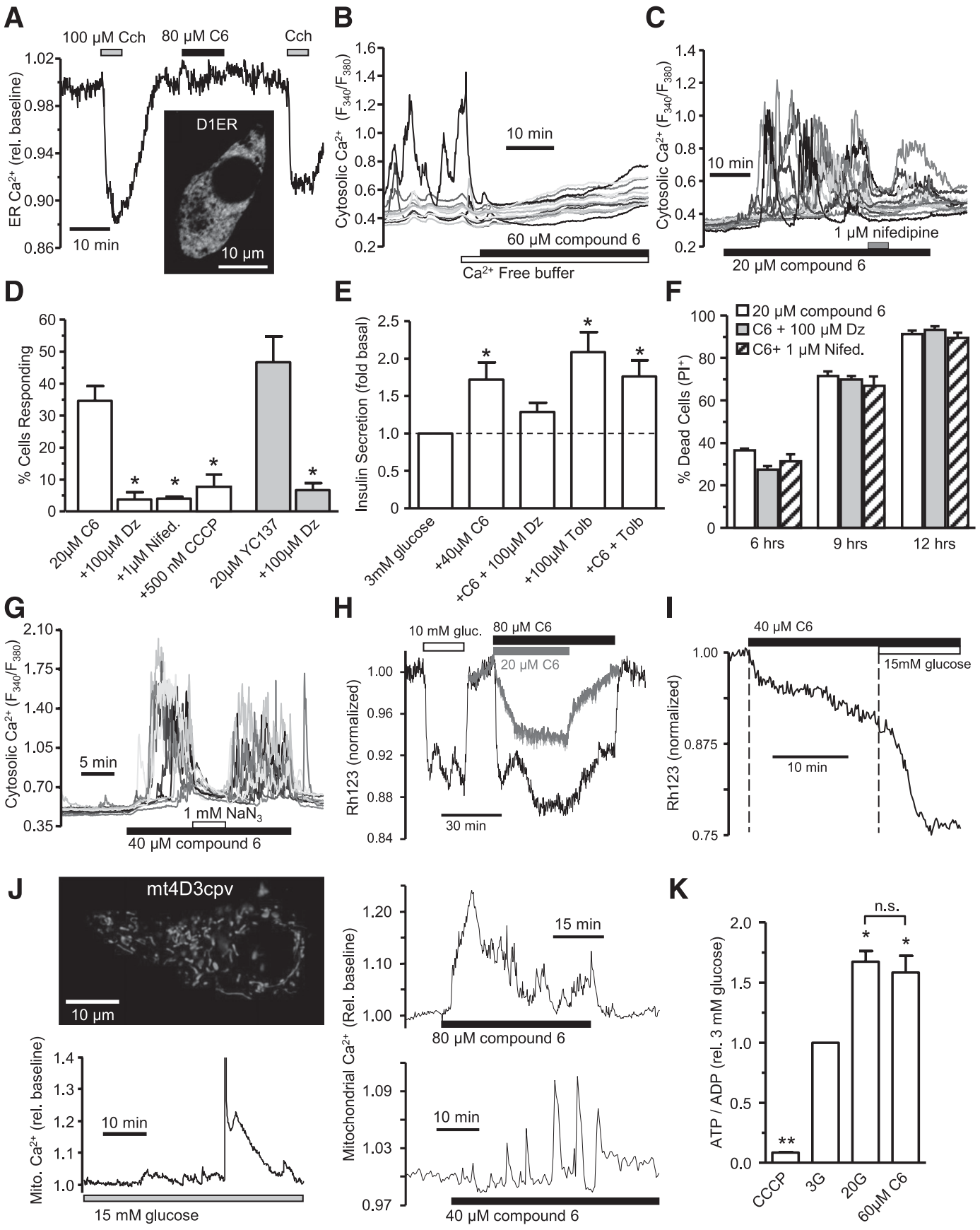

FIG. 4. Bcl-2/Bcl-x_L antagonism stimulates β-cell mitochondrial metabolism, K_{ATP}-dependent Ca^{2+} entry, and insulin secretion. *A*: Representative recording of ER Ca^{2+} changes in MIN6 β-cells exposed to C6 and carbachol (Cch) (n = 6 cells). *Inset:* MIN6 cell expressing the ER-targeted D1ER Ca^{2+} sensor. *B*: Lack of C6-induced Ca^{2+} influx in the absence of extracellular Ca^{2+}. The basally active cell illustrates the rapid loss of Ca^{2+} entry

Of note, Bcl antagonism caused an increase in the cellular ratio of ATP to ADP similar to that evoked by 20 mmol/L glucose (Fig. 4*K*). Our results demonstrate that acute inhibition of Bcl-2/Bcl-x_L promotes mitochondrial activity in β-cells, resulting in the same events activated by stimulatory glucose. These findings implicate Bcl-2 and/or Bcl-x_L in the regulation of β-cell mitochondrial physiology and suggest that one of their day-to-day roles is to suppress basal glucose metabolism.

Genetic ablation of Bcl-2 enhances β-cell glucose responses. To validate our experiments with small molecule inhibitors, we examined the importance of Bcl-2 and Bcl-x_L in β-cell function in vitro using a genetic loss-of-function approach. First, we used islets from Bcl-$2^{-/-}$ mice. These global knockout mice are approximately half the size of their wild-type or heterozygous littermates, insulin-hypersensitive, develop polycystic kidney disease, and die at various ages between 2 and 19 weeks (30) (D.S.L. and J.D.J., unpublished observations), precluding interpretable in vivo analysis of β-cell function. Nevertheless, we were able to isolate islets for in vitro analysis from a limited number of Bcl-$2^{-/-}$ mice prior to any signs of illness and compare them to islets from phenotypically normal heterozygous and wild-type littermates (31). Real-time PCR confirmed the loss of Bcl-2 expression in Bcl-$2^{-/-}$ and Bcl-$2^{+/-}$ islets relative to Bcl-$2^{+/+}$ controls, with no compensatory increase in Bcl-x_L (Fig. 5*A*). Bcl-$2^{-/-}$ and Bcl-$2^{+/-}$ β-cells showed enhanced sensitivity to a stepwise glucose ramp stimulus relative to cells from wild-type littermates (Fig. 5*B* and *C*). Intact islets from Bcl-$2^{-/-}$ mice also showed increased Ca^{2+} and metabolic NAD(P)H responses to 6 mmol/L glucose (Fig. 5*E* and *F*). In perifusion experiments, we observed significantly increased insulin secretion from Bcl-$2^{-/-}$ islets in response to 10 and 15 mmol/L glucose, compared with Bcl-$2^{+/+}$ islets (Fig. 5*G*). Loss of Bcl-2 had no effect on the responses to depolarization with KCl, further indicating a change at the level of β-cell metabolism (Fig. 5*D* and *H*). Generally, the effects on intact islets were less pronounced than those in dispersed cells, suggesting that cell–cell coupling may dampen the amplified responses of individual Bcl-$2^{-/-}$ β-cells. The intermediate augmentation of glucose-induced Ca^{2+} responses in Bcl-2 heterozygous β-cells (Fig. 5*B* and *C*) indicates that the effects were dependent on gene dosage and independent of pathological conditions that limit the number of healthy Bcl-$2^{-/-}$ mice available for study. Throughout our studies, we did not notice any obvious differences in the viability of Bcl-$2^{-/-}$ islets or β-cells in culture.

Genetic ablation of Bcl-x_L enhances β-cell glucose responses. Global deletion of Bcl-x_L is embryonically lethal (32), so to assess the specific role of Bcl-x_L, we generated tissue-specific, tamoxifen-inducible Bcl-x_L knockout (BclxβKO) mice. Bcl-x_L was knocked out in β-cells of adult animals as early as 2 to 3 days after tamoxifen administration with no compensatory change in Bcl-2 expression (Fig. 6*A*). Bcl-x_L deletion was not observed in hypothalamus (Fig. 6*B*). Using BclxβKO islet cells, we confirmed a significant molecular contribution of Bcl-x_L to C6-induced Ca^{2+} signals (Fig. 6*C*). Like Bcl-$2^{-/-}$ β-cells, BclxβKO β-cells showed significantly larger glucose-induced Ca^{2+} and NAD(P)H responses (Fig. 6*D*, *E*, and *G*), whereas Ca^{2+} responses to KCl were normal (Fig. 6*F*). These findings support a metabolic basis for the amplified Ca^{2+} responses, although we did not detect changes at the level of glucose oxidation in bulk cultures of dispersed BclxβKO islet cells (Fig. 6*H*). A modest tendency toward increases in insulin secretion was seen in BclxβKO islets perifused with 3, 6, and 10 mmol/L glucose and in mice injected with glucose in vivo, but these did not achieve statistical significance (Figs. 6*I* and 7*A*). Interestingly, glucose tolerance was nonetheless moderately improved in BclxβKO mice administered 2 g/kg glucose relative to littermate controls (Fig. 7*B*). The potentiation of β-cell Ca^{2+} signals at submaximal glucose prompted us to examine the in vivo response to a more moderate glucose challenge (0.5 g/kg), and indeed glucose tolerance was also improved under these conditions (Fig. 7*C* and *D*). This was not associated with improved insulin sensitivity (Fig. 7*E*). Together, our combined findings using chemical inhibitors and islets from knockout mice point to novel roles for both Bcl-2 and Bcl-x_L in the fine-tuning of glucose signaling in pancreatic β-cells.

Bcl-2 and Bcl-x_L affect β-cell function independently of Bax and Bak. Proapoptotic Bax and Bak have been reported to interact with two regulators of mitochondrial physiology: the voltage-dependent anion channel (VDAC) and the adenine nucleotide translocase (ANT) (33–35), but it is not clear if this occurs outside of apoptosis. Given the established roles of Bax and Bak downstream of Bcl-2/Bcl-x_L, we asked if they participate in Bcl-2/Bcl-x_L regulation of metabolism. Bax$^{-/-}$ or Bak$^{-/-}$ β-cells responded to Bcl-2/Bcl-x_L inhibition similar to wild-type β-cells (Fig. 8*A*). To conclusively exclude the involvement of Bax and Bak, we generated mice lacking both genes in their β-cells (Fig. 8*B* and *C*). Islet cells from these Bax–Bak β double-knockout (DKO) mice responded to Bcl-2/Bcl-x_L antagonism similar to islet cells from control mice (Fig. 8*D* and *E*). Together, these data establish that Bax and Bak do not mediate the effects of Bcl-2 or Bcl-x_L in β-cell function and further distinguish the physiological effects of Bcl inhibition from Bax/Bak-dependent apoptotic events.

DISCUSSION

The current study was undertaken to examine the physiological roles of endogenous prosurvival Bcl proteins in pancreatic β-cells. Using small-molecule Bcl-2/Bcl-x_L antagonists and

upon Ca^{2+} removal. *C*: Nifedipine blocks ongoing C6-induced Ca^{2+} influx (n = 14 cells). *D*: Quantification of nifedipine, diazoxide (Dz), and CCCP-mediated suppression of cytosolic Ca^{2+} responses in mouse islet cells exposed to C6 or YC137 (n = 3). *E*: Insulin secretion from dispersed islet-cells treated with C6, diazoxide, and/or tolbutamide (Tolb) (n = 5). *P < 0.05 vs. 3 mmol/L glucose control. *F*: Percentage of PI-positive mouse islet cells following culture with C6 with or without the presence of nifedipine or Dz (n = 3). *G*: Reversible inhibition of C6-induced Ca^{2+} signaling in mouse islet cells by sodium azide (NaN_3). *H* and *I*: Relative changes in $\Delta\Psi_m$ of primary mouse β-cells exposed to stimulatory glucose and the Bcl-2 antagonist C6. In panel *H*, glucose was added prior to C6. The black line is representative of 38 cells exposed to 80 μmol/L, and the superimposed red line is representative of 15 cells responding to a shorter stimulation with 20 μmol/L C6. Panel *I* illustrates the addition of glucose during the C6-induced response (representative of 17 cells). Loss of rhodamine 123 fluorescence indicates mitochondrial hyperpolarization. *J*: MIN6 β-cell expressing the mitochondrial FRET-based Ca^{2+} sensor mt4D3cpv and examples of mitochondrial Ca^{2+} fluctuations induced by glucose or Bcl-2/Bcl-x_L inhibition (n = 29 cells at 40 μmol/L C6; n = 34 cells at 80 μmol/L C6). *K*: Change in the cellular ATP-to-ADP ratio of MIN6 β-cells following 30 min culture in stimulatory 20 mmol/L glucose (20G) or in 3 mmol/L glucose with 60 μmol/L C6, relative to 3 mmol/L glucose alone. The depletion seen with CCCP reflects the metabolic pool of ATP (n = 3 cultures; *P < 0.05, **P < 0.001 vs. 3 mmol/L glucose; n.s., not significant). Data are mean ± SEM. Basal glucose is 3 mmol/L in all experiments. (A high-quality color representation of this figure is available in the online issue.)

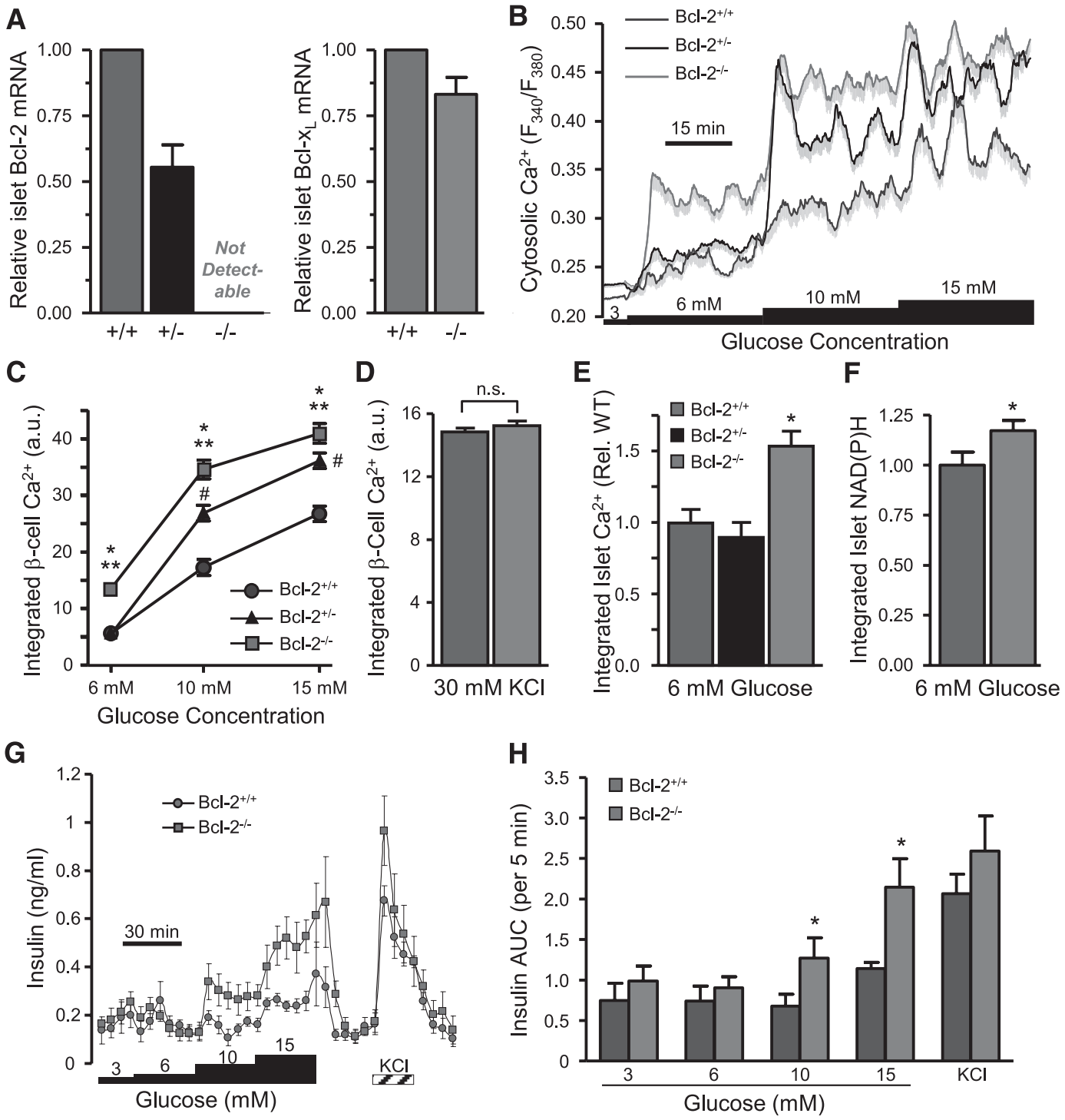

FIG. 5. Loss of Bcl-2 enhances β-cell glucose responses. *A*: Quantitative PCR (qPCR) quantification of Bcl-2 and Bcl-x$_L$ mRNA levels in islets from Bcl-2$^{+/-}$ and Bcl-2$^{-/-}$ mice relative to Bcl-2$^{+/+}$ littermates (n = 3 mice of each genotype). All data are mean ± SEM. *B*: Average cytosolic Ca^{2+} levels of dispersed islet cells from littermate Bcl-2$^{+/+}$, Bcl-2$^{+/-}$, and Bcl-2$^{-/-}$ mice. Shaded hanging bars represent SEM. *C*: Incremental area under the curve of Ca^{2+} responses (n = 98 Bcl-2$^{+/+}$ cells, n = 144 Bcl-2$^{+/-}$ cells, and n = 147 Bcl-2$^{-/-}$ cells from three mice of each genotype; *P < 0.001 Bcl-2$^{-/-}$ vs. Bcl-2$^{+/+}$, **P < 0.01 Bcl-2$^{-/-}$ vs. Bcl-2$^{+/-}$, and #P < 0.05 Bcl-2$^{+/-}$ vs. Bcl$^{+/+}$). *D*: Integrated cytosolic Ca^{2+} responses of Bcl-2$^{-/-}$ and Bcl-2$^{+/+}$ β-cells depolarized with 30 mmol/L KCl (n = 87 Bcl-2$^{+/+}$ cells and 130 Bcl-2$^{-/-}$ cells from three mice of each genotype). n.s., not significant. *E* and *F*: Integrated Ca^{2+} and NAD(P)H autofluorescence increases of intact islets, normalized to Bcl-2$^{+/+}$ control (panel *E*: n = 16 Bcl-2$^{+/+}$ islets; n = 20 Bcl-2$^{+/-}$ islets; n = 21 Bcl-2$^{-/-}$ islets; and panel *F*: n = 16 Bcl-2$^{+/+}$ islets; n = 17 Bcl-2$^{-/-}$ islets; three mice of each genotype; *P < 0.05, **P < 0.01 vs. Bcl-2$^{+/+}$). *G*: Insulin secretion profiles of perifused islets from 5–7-week-old Bcl-2$^{+/+}$ and Bcl-2$^{-/-}$ mice. *H*: Quantified area under the curve of insulin secretion profiles in panel *G* (n = 5; *P < 0.05 vs. Bcl-2$^{+/+}$). a.u., arbitrary units. (A high-quality color representation of this figure is available in the online issue.)

islets from KO mice, we provide the first loss-of-function evidence that Bcl-2 and Bcl-x$_L$ acutely affect mitochondrial function, Ca^{2+} homeostasis, and insulin secretion. A previous report described apoptosis sensitivity in mice in which Bcl-x$_L$ was deleted in embryonic β-cells, but did not provide information on glucose homeostasis or β-cell physiology (5). The effects of the chemical inhibitors, which target both Bcl-2 and Bcl-x$_L$, were partially distinct and generally more

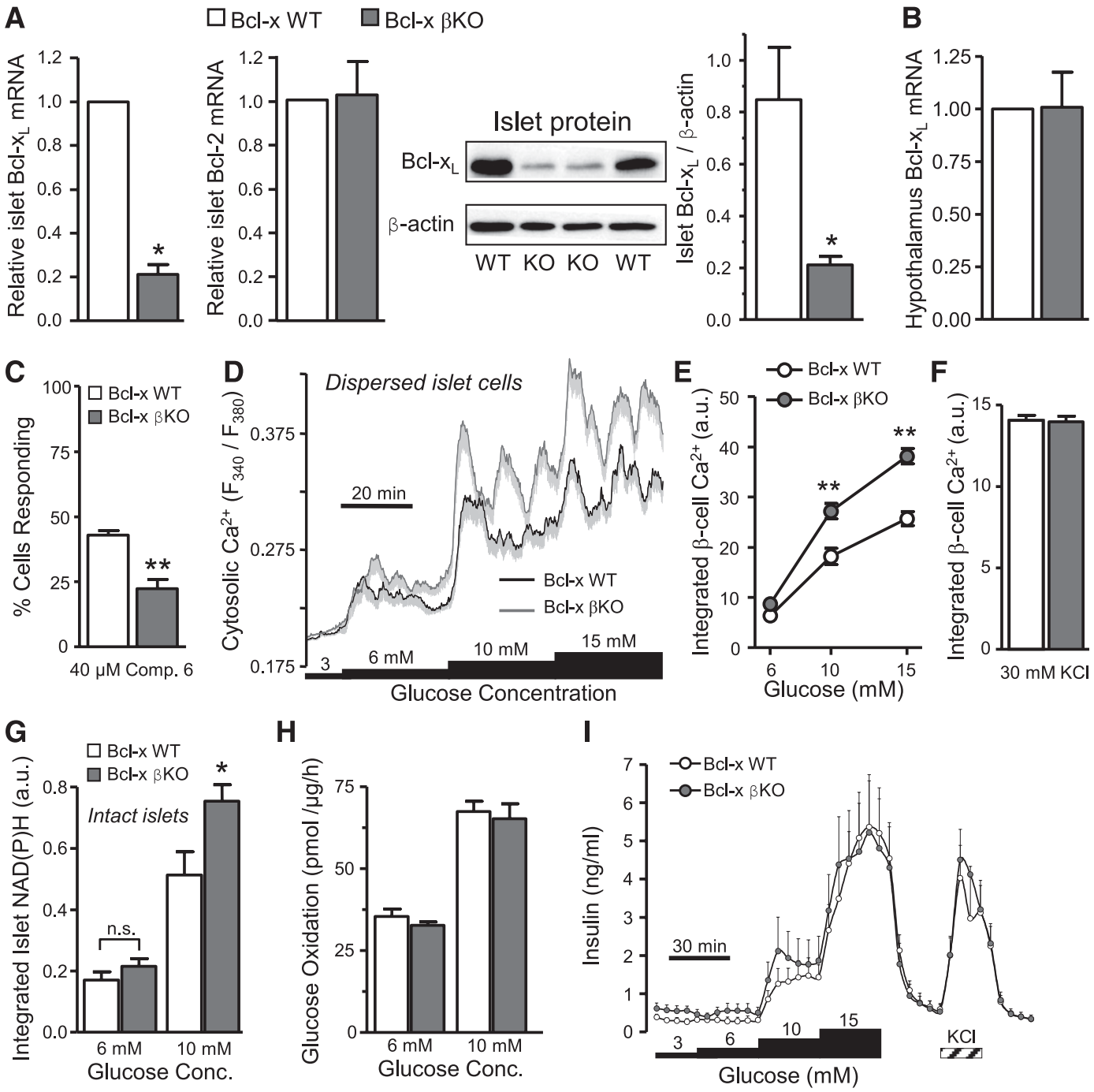

FIG. 6. Inducible deletion of Bcl-x_L enhances β-cell glucose signaling. *A*: Quantification of Bcl-x_L and Bcl-2 mRNA levels by quantitative PCR (qPCR) (n = 3) and Bcl-x_L protein by Western blot (n = 6) in islets from tamoxifen-injected Bcl-$x^{flox/flox}$:Pdx1-CreER (Bcl-x βKO) mice relative to islets from tamoxifen-injected littermate Bcl-$x^{flox/flox}$ (Bcl-x WT) mice (data are mean ± SEM; *P < 0.05). *B*: qPCR quantification of Bcl-x_L mRNA in hypothalamus from Bcl-x_L WT and KO mice (n = 3). *C*: Percentage of Bcl-x WT and βKO islet cells responding to small-molecule Bcl inhibition (n = 5 mice of each genotype; **P < 0.001 vs. Bcl-x WT). *D*: Average cytosolic Ca^{2+} responses of Bcl-x βKO and WT β-cells stimulated with increasing glucose concentrations (Conc.). Shaded hanging bars represent SEM. *E*: Incremental area under the curve of Ca^{2+} responses. *F*: Integrated Ca^{2+} responses of Bcl-x KO and Bcl-x WT β-cells depolarized with 30 mmol/L KCl (n = 66 Bcl-x WT cells; n = 73 Bcl-x KO cells; three mice per genotype; **P < 0.001). *G*: Integrated NAD(P)H increases of intact islets following glucose stimulation (n = 11 islets, two mice of each genotype; *P < 0.05). *H*: Glucose oxidation rates in cultures of dispersed Bcl-x_L WT and KO islet cells (n = 4). *I*: Insulin secretion from perifused Bcl-x WT and KO islets (n = 5). a.u., arbitrary units. (A high-quality color representation of this figure is available in the online issue.)

robust than the genetic ablation of either protein individually. It is likely that combined tissue-specific deletion of Bcl-2 and Bcl-x will be required to mimic the effects of the inhibitors on basal β-cell activity and viability. Our work demonstrates new physiological roles for two proteins previously presumed to function mainly in the control of apoptosis.

Sustained cytosolic Ca^{2+} rises and insulin release following glucose stimulation rely heavily on mitochondrial ATP synthesis, K_{ATP} channel-dependent β-cell depolarization, and voltage-gated Ca^{2+} influx (28). In this study, we report that acute coinhibition of antiapoptotic Bcl-2 and Bcl-x_L stimulates an identical cascade of events culminating

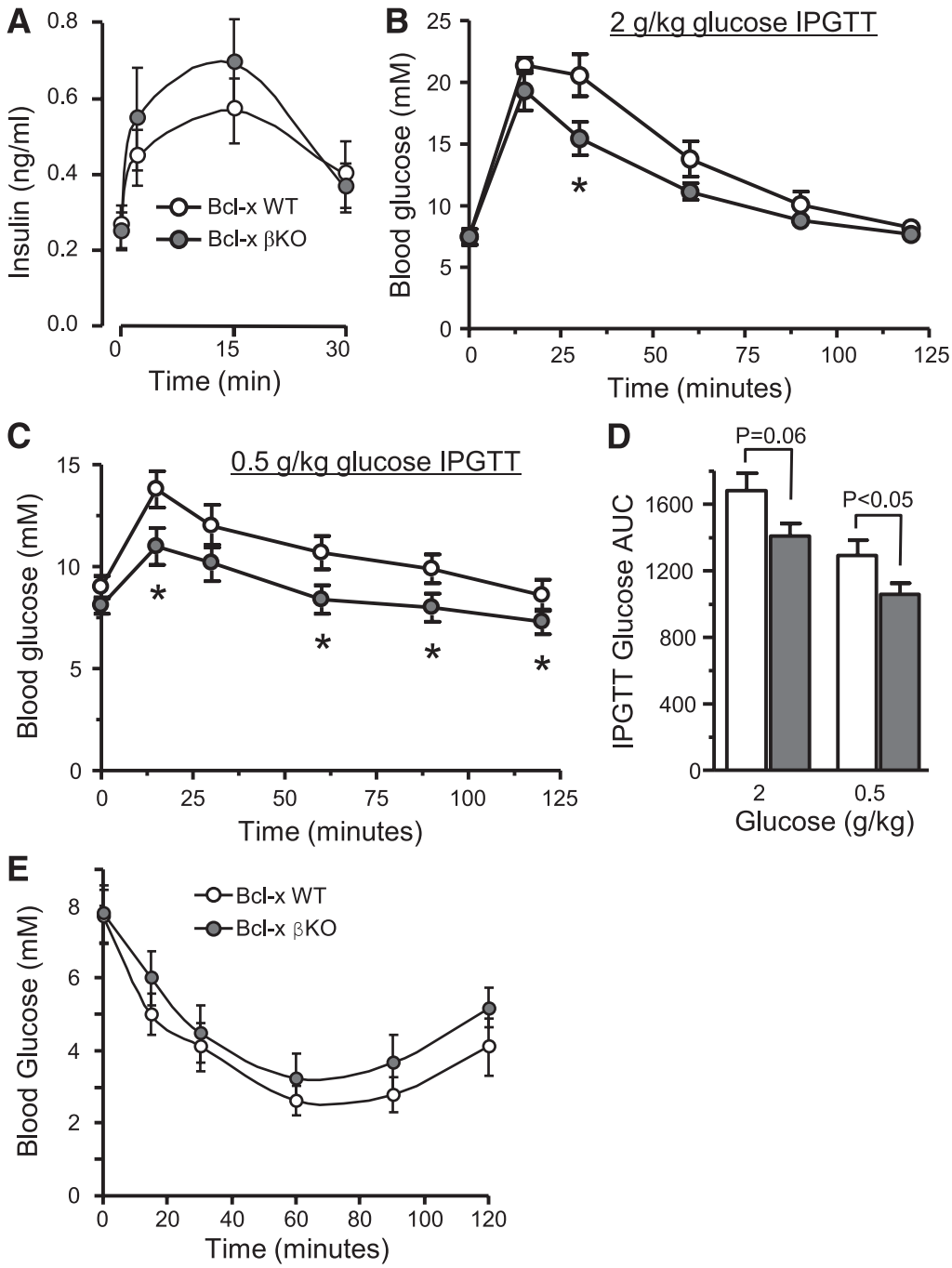

FIG. 7. Improved glucose tolerance in Bcl-x βKO mice. *A*: In vivo insulin secretion following intraperitoneal injection of 2 g/kg glucose in 10–12-week-old Bcl-x WT and βKO littermate mice ($n = 5$). *B* and *C*: Intraperitoneal glucose tolerance tests of Bcl-x βKO and WT mice using 2 and 0.5 g/kg glucose doses ($n = 7$ and $n = 8$, respectively; *$P < 0.05$). *D*: Area under the curve analysis of glucose profiles in panels *B* and *C*. *E*: Insulin tolerance test of Bcl-x WT and βKO mice ($n = 5$). IPGTT, intraperitoneal glucose tolerance test; mM, mmol/L. (A high-quality color representation of this figure is available in the online issue.)

in insulin secretion. Moreover, genetic deletion of Bcl-2 or Bcl-x_L increased the in vitro β-cell responses to glucose and improved in vivo glucose tolerance of the islet-specific Bcl-x_L KO mice. Our experiments suggest that this involves amplification of β-cell glucose metabolism and thus that Bcl-2 and Bcl-x_L restrict β-cell metabolic activity. Our findings conceptually agree with a previous study in which mice overexpressing Bcl-x_L 10-fold under the control of the rat insulin promoter exhibited impaired β-cell oxidative metabolism and glucose intolerance (9). Several groups have overexpressed Bcl-2 in pancreatic islets as part of efforts to block apoptosis, but we are only aware of a few studies that examined the impact on β-cell function, and these reported no impairment of insulin secretion (36,37). This could be interpreted as evidence for a saturation effect whereby excess levels of Bcl-2 protein do not negatively affect the stoichiometry of complexes associated with the metabolic machinery. Alternatively, the lower fraction of mitochondria-localized Bcl-2 relative to Bcl-x_L (Fig. 3) might require that correspondingly larger amounts

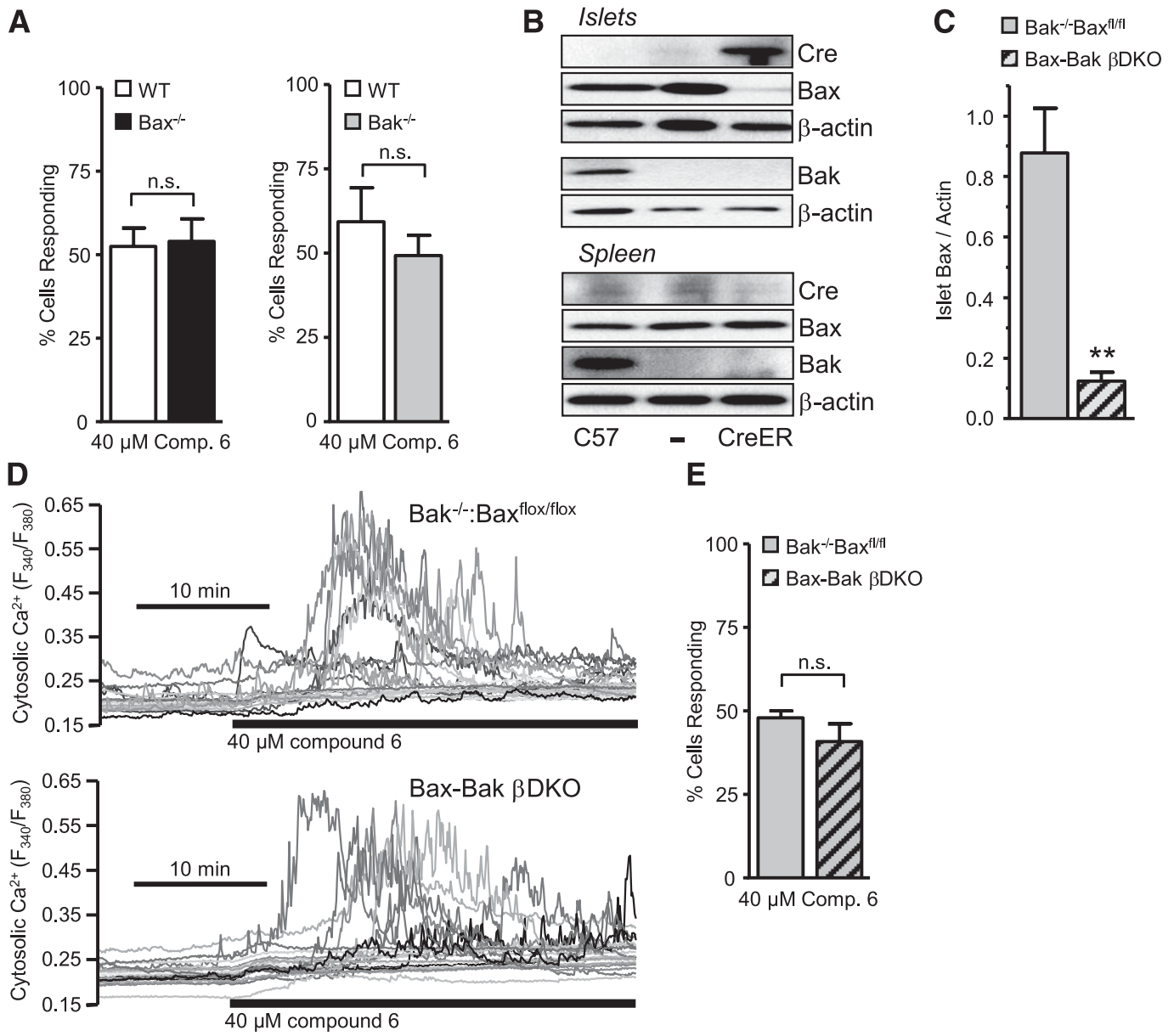

FIG. 8. Effect of Bcl antagonism in Bax, Bak, and Bcl-x_L–deficient islet cells. *A*: Percentage of islet cells responding to Bcl antagonism in preparations from $Bax^{-/-}$ (*left*), $Bak^{-/-}$ (*right*), and their wild-type control mice (n = 3 mice). Data are mean ± SEM. Basal glucose was 3 mmol/L in all experiments. *B*: Western blot demonstrating global Bak deficiency and islet specific Bax knockout in tamoxifen-injected $Bak^{-/-}$:$Bax^{flox/flox}$:Pdx1-CreER (Bax-Bak βDKO) mice relative to tamoxifen-injected $Bak^{-/-}$:$Bax^{flox/flox}$ and C57BL6/J (C57) mice. *C*: Bax protein levels were reduced by 85% in Bax-Bak βDKO islets (n = 6; **P < 0.001 vs. $Bak^{-/-}$:$Bax^{flox/flox}$). *D*: Comparable Bcl inhibitor-induced Ca^{2+} responses in groups of $Bak^{-/-}Bax^{flox/flox}$ and Bax-Bak βDKO islet cells. *E*: Percentage of Bak-Bax βDKO and $Bak^{-/-}$:$Bax^{flox/flox}$ islet-cells responding to Bcl inhibition (n = 3 mice of each genotype). (A high-quality color representation of this figure is available in the online issue.)

of Bcl-2 are expressed to achieve detectable metabolic suppression.

We considered that antagonizing Bcl-2/Bcl-x_L might free Bax and/or Bak to indirectly activate mitochondria, possibly by affecting ANT or VDAC (33–35). We tested and eliminated this possibility using Bax KO, Bak KO, and Bax/Bak DKO islet cells. Work from the Danial group (3,38) is consistent with an alternative indirect model whereby Bcl-2 and/or Bcl-x_L might sequester Bad and limit its promotion of glucokinase activity. Bcl-2 and Bcl-x_L have not been detected in the Bad/glucokinase complex, but reducing their binding to Bad might release this brake on β-cell metabolism from afar. In preliminary studies in MIN6 cells, Bcl inhibition did not change Bad levels or phosphorylation within 60 min, the timescale corresponding to the acute Ca^{2+} signals and metabolic effects. Preliminary studies in Bcl-x_L KO islets revealed 58% increase in serine 155 phosphorylation, with no significant effects on the phosphorylation of Bad at serine 136 or serine 112. Thus, phosphorylation-dependent functions of Bad do not appear acutely involved in the effects of Bcl antagonism. However, a more chronic contribution from the Bad/glucokinase axis following chronic Bcl protein loss remains a possibility that might promote the amplification of insulin secretion in stimulatory glucose that is not apparent acutely following inhibition with small molecules.

Our data also allow for a model whereby Bcl proteins directly affect mitochondrial proteins in the β-cell,

provided such interactions are changed by Bcl antagonists. Studies of the antiapoptotic activities of Bcl-2 and Bcl-x_L have reported that they can interact with mitochondrial ANT and VDAC via their BH4 domains (35). We have found that a cell-permeant Bcl-x_L BH4 domain peptide triggers cytosolic and mitochondrial Ca^{2+} fluctuations in β-cells (D.S.L. and J.D.J. unpublished observations). This could result from direct mitochondrial actions of the BH4 domain and/or ER Ca^{2+} release (39). Of note, it was recently reported that Bcl-x_L can lower acetyl-CoA levels independently of Bax and Bak (40). Another study suggested that Bcl-x_L suppresses O_2 consumption, although promoting ATP synthesis in neurons by interacting with the mitochondrial F_1F_0 ATPase (8), indicating that Bcl-x_L can have opposing metabolic effects in a cell. Conceivably, changes in the relative contributions of these effects may shape the net metabolic impact of Bcl-x_L in a given cell type and might complicate the analysis of complex mechanisms such as insulin secretion that involve multiple metabolic pathways.

Our finding that antiapoptotic Bcl-2 family proteins can modulate β-cell function has intriguing implications for our understanding of the pathophysiology of diabetes. The signal transduction machinery of β-cells is optimized for maximal delivery of glycolytic intermediates for oxidative phosphorylation (41). However, β-cells are remarkably sensitive to the deleterious effects of reactive oxygen species (42). Metabolic suppression may provide a means by which Bcl proteins protect pancreatic β-cells against metabolic stress. One might also speculate that the reduction in Bcl-2 and Bcl-x_L seen under prodiabetic conditions (4,43–45) can affect β-cell function. In this regard, it is noteworthy that insulin hypersecretion is an early marker of human diabetes (46), and chronic hyperinsulinemia a persistent feature of diabetic animal models, including the Zucker Diabetic Fatty rat (47), which has 70% less Bcl-2 protein (48). In extension of this, our results suggest caution may be prudent in efforts to treat diabetes by augmenting β-cell metabolic flux using agents such as glucokinase activators (49).

In summary, we demonstrate novel roles of endogenous antiapoptotic Bcl proteins in the physiology of pancreatic β-cells. Specifically, our data suggest that endogenous Bcl-2 and Bcl-x_L suppress the β-cell response to glucose. Our findings add to emerging evidence that places Bcl family proteins at the intersection of β-cell function and survival. The involvement of apoptosis-regulating proteins in the normal function of primary cells promises to provide fertile grounds for future insights into the pathophysiology of diabetes and other diseases.

ACKNOWLEDGMENTS

This work was supported by operating grants from the Canadian Institutes of Health Research (CIHR) (MOP-86559 to J.D.J. and MOP-119537 to D.S.L.). J.D.J. was supported by salary awards from the CIHR, the Juvenile Diabetes Research Foundation (JDRF), the Canadian Diabetes Association (CDA), and the Michael Smith Foundation for Health Research (MSFHR). D.S.L. received fellowship support from the JDRF, the Carlsberg Foundation, CDA, and the MSFHR.

No potential conflicts of interest relevant to this article were reported.

D.S.L. designed experiments, performed research, and wrote the manuscript. S.A.W., S.B.W., and V.V.S. performed research, contributed to discussion, and reviewed and edited the manuscript. F.T. performed research. X.H. performed research. M.F.A. contributed to discussion and reviewed and edited manuscript. J.D.J. designed research and wrote the manuscript. J.D.J. is the guarantor of this work and, as such, had full access to all the data in the study and takes responsibility for the integrity of the data and the accuracy of the data analysis.

The authors thank Dr. Douglas Melton, Harvard University, for the Pdx1-CreER mice and Dr. You-Wen He, Duke University, for the Bcl-x^{flox} mice. The authors also thank Dr. Atsushi Miyawaki, RIKEN Japan, for the MiCy-DEVD-mKO probe; Dr. Roger Tsien, University of California San Diego, and Dr. Amy Palmer, University of Colorado, for the mt4D3cpv and D1ER Ca^{2+} sensors; and Karen Groden, Suzen Lines, and the University of British Columbia rederivation facility for help with husbandry of the Bcl-2 mice.

REFERENCES

1. Petros AM, Olejniczak ET, Fesik SW. Structural biology of the Bcl-2 family of proteins. Biochim Biophys Acta 2004;1644:83–94
2. Youle RJ, Strasser A. The BCL-2 protein family: opposing activities that mediate cell death. Nat Rev Mol Cell Biol 2008;9:47–59
3. Danial NN, Walensky LD, Zhang CY, et al. Dual role of proapoptotic BAD in insulin secretion and beta cell survival. Nat Med 2008;14:144–153
4. Emamaullee JA, Shapiro AM. Interventional strategies to prevent beta-cell apoptosis in islet transplantation. Diabetes 2006;55:1907–1914
5. Carrington EM, McKenzie MD, Jansen E, et al. Islet beta-cells deficient in Bcl-xL develop but are abnormally sensitive to apoptotic stimuli. Diabetes 2009;58:2316–2323
6. Rong Y, Distelhorst CW. Bcl-2 protein family members: versatile regulators of calcium signaling in cell survival and apoptosis. Annu Rev Physiol 2008; 70:73–91
7. Vander Heiden MG, Thompson CB. Bcl-2 proteins: regulators of apoptosis or of mitochondrial homeostasis? Nat Cell Biol 1999;1:E209–E216
8. Alavian KN, Li H, Collis L, et al. Bcl-xL regulates metabolic efficiency of neurons through interaction with the mitochondrial F1FO ATP synthase. Nat Cell Biol 2011;13:1224–1233
9. Zhou YP, Pena JC, Roe MW, et al. Overexpression of Bcl-x(L) in beta-cells prevents cell death but impairs mitochondrial signal for insulin secretion. Am J Physiol Endocrinol Metab 2000;278:E340–E351
10. Ou D, Wang X, Metzger DL, et al. Synergistic inhibition of tumor necrosis factor-related apoptosis-inducing ligand-induced apoptosis in human pancreatic beta cells by Bcl-2 and X-linked inhibitor of apoptosis. Hum Immunol 2005;66:274–284
11. Saldeen J. Cytokines induce both necrosis and apoptosis via a common Bcl-2-inhibitable pathway in rat insulin-producing cells. Endocrinology 2000;141:2003–2010
12. Luciani DS, Ao P, Hu X, Warnock GL, Johnson JD. Voltage-gated Ca(2+) influx and insulin secretion in human and mouse beta-cells are impaired by the mitochondrial Na(+)/Ca(2+) exchange inhibitor CGP-37157. Eur J Pharmacol 2007;576:18–25
13. Luciani DS, Misler S, Polonsky KS. Ca^{2+} controls slow NAD(P)H oscillations in glucose-stimulated mouse pancreatic islets. J Physiol 2006;572:379–392
14. Luciani DS, Gwiazda KS, Yang TL, et al. Roles of IP3R and RyR Ca2+ channels in endoplasmic reticulum stress and beta-cell death. Diabetes 2009;58:422–432
15. Saeedi R, Parsons HL, Wambolt RB, et al. Metabolic actions of metformin in the heart can occur by AMPK-independent mechanisms. Am J Physiol Heart Circ Physiol 2008;294:H2497–H2506
16. Allard MF, Schönekess BO, Henning SL, English DR, Lopaschuk GD. Contribution of oxidative metabolism and glycolysis to ATP production in hypertrophied hearts. Am J Physiol 1994;267:H742–H750
17. Gu G, Dubauskaite J, Melton DA. Direct evidence for the pancreatic lineage: NGN3+ cells are islet progenitors and are distinct from duct progenitors. Development 2002;129:2447–2457
18. Zhang N, He YW. The antiapoptotic protein Bcl-xL is dispensable for the development of effector and memory T lymphocytes. J Immunol 2005;174: 6967–6973
19. Johnson JD, Ford EL, Bernal-Mizrachi E, et al. Suppressed insulin signaling and increased apoptosis in CD38-null islets. Diabetes 2006;55:2737–2746
20. Luciani DS, Johnson JD. Acute effects of insulin on beta-cells from transplantable human islets. Mol Cell Endocrinol 2005;241:88–98

21. Real PJ, Cao Y, Wang R, et al. Breast cancer cells can evade apoptosis-mediated selective killing by a novel small molecule inhibitor of Bcl-2. Cancer Res 2004;64:7947–7953
22. Enyedy IJ, Ling Y, Nacro K, et al. Discovery of small-molecule inhibitors of Bcl-2 through structure-based computer screening. J Med Chem 2001;44:4313–4324
23. Kaufmann T, Schlipf S, Sanz J, Neubert K, Stein R, Borner C. Characterization of the signal that directs Bcl-x(L), but not Bcl-2, to the mitochondrial outer membrane. J Cell Biol 2003;160:53–64
24. Akao Y, Otsuki Y, Kataoka S, Ito Y, Tsujimoto Y. Multiple subcellular localization of bcl-2: detection in nuclear outer membrane, endoplasmic reticulum membrane, and mitochondrial membranes. Cancer Res 1994;54:2468–2471
25. White C, Li C, Yang J, et al. The endoplasmic reticulum gateway to apoptosis by Bcl-X(L) modulation of the InsP3R. Nat Cell Biol 2005;7:1021–1028
26. Chen R, Valencia I, Zhong F, et al. Bcl-2 functionally interacts with inositol 1,4,5-trisphosphate receptors to regulate calcium release from the ER in response to inositol 1,4,5-trisphosphate. J Cell Biol 2004;166:193–203
27. Palmer AE, Jin C, Reed JC, Tsien RY. Bcl-2-mediated alterations in endoplasmic reticulum Ca2+ analyzed with an improved genetically encoded fluorescent sensor. Proc Natl Acad Sci USA 2004;101:17404–17409
28. Misler S, Barnett DW, Gillis KD, Pressel DM. Electrophysiology of stimulus-secretion coupling in human beta-cells. Diabetes 1992;41:1221–1228
29. Palmer AE, Giacomello M, Kortemme T, et al. Ca2+ indicators based on computationally redesigned calmodulin-peptide pairs. Chem Biol 2006;13:521–530
30. Veis DJ, Sorenson CM, Shutter JR, Korsmeyer SJ. Bcl-2-deficient mice demonstrate fulminant lymphoid apoptosis, polycystic kidneys, and hypopigmented hair. Cell 1993;75:229–240
31. Sorenson CM, Rogers SA, Korsmeyer SJ, Hammerman MR. Fulminant metanephric apoptosis and abnormal kidney development in bcl-2-deficient mice. Am J Physiol 1995;268:F73–F81
32. Motoyama N, Wang F, Roth KA, et al. Massive cell death of immature hematopoietic cells and neurons in Bcl-x-deficient mice. Science 1995;267:1506–1510
33. Cheng EH, Sheiko TV, Fisher JK, Craigen WJ, Korsmeyer SJ. VDAC2 inhibits BAK activation and mitochondrial apoptosis. Science 2003;301:513–517
34. Marzo I, Brenner C, Zamzami N, et al. Bax and adenine nucleotide translocator cooperate in the mitochondrial control of apoptosis. Science 1998;281:2027–2031
35. Tsujimoto Y, Shimizu S. VDAC regulation by the Bcl-2 family of proteins. Cell Death Differ 2000;7:1174–1181
36. Rabinovitch A, Suarez-Pinzon W, Strynadka K, et al. Transfection of human pancreatic islets with an anti-apoptotic gene (bcl-2) protects beta-cells from cytokine-induced destruction. Diabetes 1999;48:1223–1229
37. Dupraz P, Rinsch C, Pralong WF, et al. Lentivirus-mediated Bcl-2 expression in betaTC-tet cells improves resistance to hypoxia and cytokine-induced apoptosis while preserving in vitro and in vivo control of insulin secretion. Gene Ther 1999;6:1160–1169
38. Danial NN, Gramm CF, Scorrano L, et al. BAD and glucokinase reside in a mitochondrial complex that integrates glycolysis and apoptosis. Nature 2003;424:952–956
39. Rong YP, Bultynck G, Aromolaran AS, et al. The BH4 domain of Bcl-2 inhibits ER calcium release and apoptosis by binding the regulatory and coupling domain of the IP3 receptor. Proc Natl Acad Sci USA 2009;106:14397–14402
40. Yi CH, Pan H, Seebacher J, et al. Metabolic regulation of protein N-alpha-acetylation by Bcl-xL promotes cell survival. Cell 2011;146:607–620
41. Sekine N, Cirulli V, Regazzi R, et al. Low lactate dehydrogenase and high mitochondrial glycerol phosphate dehydrogenase in pancreatic beta-cells. Potential role in nutrient sensing. J Biol Chem 1994;269:4895–4902
42. Thomas HE, McKenzie MD, Angstetra E, Campbell PD, Kay TW. Beta cell apoptosis in diabetes. Apoptosis 2009;14:1389–1404
43. Mizuno N, Yoshitomi H, Ishida H, et al. Altered bcl-2 and bax expression and intracellular Ca2+ signaling in apoptosis of pancreatic cells and the impairment of glucose-induced insulin secretion. Endocrinology 1998;139:1429–1439
44. Johnson JD, Ahmed NT, Luciani DS, et al. Increased islet apoptosis in Pdx1+/- mice. J Clin Invest 2003;111:1147–1160
45. Huang Q, Bu S, Yu Y, et al. Diazoxide prevents diabetes through inhibiting pancreatic beta-cells from apoptosis via Bcl-2/Bax rate and p38-beta mitogen-activated protein kinase. Endocrinology 2007;148:81–91
46. Simonson DC. Hyperinsulinemia and its sequelae. Horm Metab Res Suppl 1990;22:17–25
47. Zhou YP, Cockburn BN, Pugh W, Polonsky KS. Basal insulin hypersecretion in insulin-resistant Zucker diabetic and Zucker fatty rats: role of enhanced fuel metabolism. Metabolism 1999;48:857–864
48. Shimabukuro M, Wang MY, Zhou YT, Newgard CB, Unger RH. Protection against lipoapoptosis of beta cells through leptin-dependent maintenance of Bcl-2 expression. Proc Natl Acad Sci USA 1998;95:9558–9561
49. Grimsby J, Sarabu R, Corbett WL, et al. Allosteric activators of glucokinase: potential role in diabetes therapy. Science 2003;301:370–373